Two-Phase Flow in Porous Media: Property Identification and Model Validation

Raghavendra Kulkarni and A. Ted Watson
Dept. of Chemical Engineering, Texas A&M University, College Station, TX 77843

Jan-Erik Nordtvedt and André Sylte
RF-Rogaland Research, N-5008 Bergen, Norway

The experimental design and analysis of two-phase dynamic displacement experiments are investigated, with particular attention to incorporating measured saturation distributions. Pressure drops and saturation distributions measured with displacement experiments using multiple flow-rate injection rates can provide accurate estimates of relative permeability and capillary pressure functions over broad ranges of fluid saturations. Successful reconciliation of measured saturation distributions and pressure drops establishes an experimental validation of the Darcy model for two-phase flow in porous media.

Introduction

The mathematical modeling and simulation of the flow of fluids through porous media are important for designing and controlling a number of industrial processes, including the production of fluids from underground reservoirs and remediation of underground water resources. The simulation of fluid flow is typically carried out using constitutive and conservation relations based on a macroscopic representation of porous media. In the macroscopic representation, the fluid states correspond to local volume averages and are continuous functions of position and time. The use of the macroscopic scale eliminates the necessity of knowing the detailed, microscopic geometry of the media, information which is basically unavailable. The properties of the media are *effective* properties, representing local volume averages, which are defined by the constitutive relations.

The flow of multiple immiscible fluid phases through porous media has been essentially universally described by a Darcy equation and equation of continuity for each fluid phase:

$$\vec{v}_i = -\frac{\mathbf{K}_i}{\mu_i}\cdot(\nabla p_i - \rho_i \vec{g}), \tag{1}$$

$$\frac{\partial(\phi \rho_i s_i)}{\partial t} = -\nabla\cdot(\rho_i \vec{v}_i). \tag{2}$$

The differences between the pressures of the two fluid phases are related by the capillary pressure

$$p_{c_{ij}}(s_i) = p_i(s_i) - p_j(s_i) \tag{3}$$

and the saturations are related by

$$\Sigma s_i = 1 \tag{4}$$

The permeability of each fluid phase is typically represented as the product of the absolute permeability, as defined for single-phase flow, and the relative permeability of that phase

$$\mathbf{K}_i = \mathbf{K} k_{ri}(s_i) \tag{5}$$

Presumably, spatial dependence can largely be taken into account with the absolute permeability, so that the relative permeability functions may be taken to be uniform over a relatively larger region of the medium.

Does the mathematical model represented by Eqs. 1–5, together with boundary and initial conditions, provide a good description of multiphase flow in porous media? That is, for a porous medium, are there a set of properties so that the mathematical model accurately predicts the fluid states? In spite of the universality of the model, there are very few experimental validations, and none that includes validation of fluid states *within* the porous medium.

Correspondence concerning this article should be addressed to A. T. Watson.
Current address of R. Kulkarni: GeoQuest Interpretation and Computing Services, 4100 Spring Valley Road, Suite 600, Dallas, TX 75244.

The Darcy equation is well established for single-phase flow (Slattery, 1969; Whitaker, 1969, 1986a; Larson, 1981), notwithstanding the fact that the permeability may not be accurately resolved as a function of position with current experimental methods. Theoretical support exists for the extension of that constitutive equation to two-phase flow (see Slattery, 1970; Larson, 1981; Whitaker, 1986b). Whitaker (1986b) developed an expression that corresponds to Eq. 1, but contains an additional term that reflects the viscous drag of one fluid upon the other. The relative significance of such a term is not known. Even if the Darcy equation is valid, the actual functional dependence of the relative permeabilities remains a problem. The relative permeabilities are taken to be nondecreasing, nonnegative monotonic functions of their own saturation that are equal to zero at irreducible saturations. However, additional dependencies are expected, as the relative permeabilities do seem to depend on saturation history, capillary number, and viscosity ratio (see Odeh, 1959; Wilkinson, 1984; Constantinides and Payatakes, 1996). Experimental methods to assess such effects, and databases to use to develop predictions of such effects on the relative permeability and/or capillary pressure properties, would be most desirable. However, there are few, if any, definitive experimental studies.

The primary reason for this seems to be that the conventional methods for determining relative permeabilities from laboratory experiments (Leverett, 1940; Johnson et al., 1959) often do not provide accurate estimates of relative permeabilities. The main reasons for this are discussed in some detail in the "Analysis of Experimental Data" section. Most notably, the role of the mathematical model of the experiment in estimating relative permeabilities apparently was not recognized until after the conventional methods were established (Archer and Wong, 1973; Sigmund and McCaffery, 1979), and only recently have the suitability of various assumptions in the estimation processes been assessed (Kerig and Watson, 1986; Richmond and Watson, 1990).

Our main objective is to develop methodology to determine porous media properties with sufficient accuracy to generate useful databases. This will enable better understanding and prediction of various physical effects on the relative permeabilities. It is recognized that, because the relative permeabilities are effective properties which are defined within Darcy's Law, that relation must be assumed in order to estimate those properties. Obviously, experimental confirmation of that constitutive relation is highly desirable. Like any constitutive relation, Darcy's Law cannot be proven experimentally. However, evidence for the relation is established when predictions with Darcy's Law are consistent with experimental observations. This issue is discussed in greater detail in the "Validation" section.

The relatively recent developments in the use of CT scanning (Wellington and Vinegar, 1987; Withjack, 1988) and nuclear magnetic resonance imaging (MRI) (Watson and Chang, 1997) for probing porous media have provided exciting new opportunities for investigating multiphase flow in porous media. Although the conventional methods for estimating relative permeabilities are based on measurements outside the porous media, such as production and pressure drop, we now have the opportunity to use measurements of fluid states within samples to obtain more accurate estimates of relative permeability. Furthermore, these *in-situ* data provide significant new opportunities for assessing mathematical models used to describe multiphase flow.

In this paper, the use of measurements of saturation distributions for obtaining estimates of relative permeabilities and capillary pressure from laboratory experiments is explored. Since this methodology may prove valuable for routine determination of those properties, we have investigated the actual design of the experiments and performed a study to assess the improvements in the accuracy of estimates of the properties that may be obtained as compared to conventional experimental measurements. Then, we have evaluated the extent to which the mathematical model for two-phase flow describes measured fluid states.

Analysis of Experimental Data

In this section we provide some background about the methodology used to estimate the porous media properties. We show the role of the mathematical model in the estimation process and provide some perspective on the conventional methods for determining relative permeabilities. We then discuss the validation of the mathematical model with experimental data.

Estimation of properties

The relative permeabilities are essentially defined within the Darcy equations, so they must be determined through solution of some inverse problem whereby functions of the state variables are observed during an experiment and the properties inferred through the mathematical model for the experiment. This is a particularly challenging inverse problem for several reasons. The mathematical model is a set of nonlinear partial differential and algebraic equations for which closed-form solutions are generally not available. The properties to be determined are functions of a state (dependent) variable, namely, saturation; they are taken to be smooth, monotonic, and nonnegative, but the functional representations are otherwise unknown.

Traditionally, two different methods have been used to estimate the relative permeability. These two methods are based on certain simplifications of the Darcy model for which closed-form solutions can be obtained.

The first method is the steady-state experiment, in which two fluid phases are injected simultaneously into the sample at a succession of different constant rates (Leverett, 1940). Measurements of the pressure drop and average saturation are made after a steady-state has been achieved at each rate. If it is assumed that the porous medium is spatially uniform, there are no capillary pressure effects, and fluids are incompressible, each Darcy equation can be integrated and the relative permeability for each phase calculated and assigned to the value of the average saturation.

The second method is the conventional dynamic displacement experiment, in which a single fluid is injected at a constant flow rate into a sample initially saturated with the other fluid phase. The transient pressure drop and production are measured. With the same stated assumptions, closed-form solutions can be obtained for the transient pressure drop and production. Using estimates of the derivatives of the mea-

sured data, relative permeability values corresponding to saturation values at the exit face are calculated (Johnson et al., 1959).

These two methods suffer from a number of problems. They are explicit (or direct) methods in that the properties are directly calculated from the measured data. Consequently, they only provide for calculation of relative permeability points, although estimates of the entire functions are desired. In the steady-state method, it can take a very long time to establish equilibrium, so determination of a sufficient number of relative permeability values to specify the relative permeability functions is essentially out of the question. Furthermore, capillary pressure effects can lead to a distribution of saturation within the sample (Chang et al., 1997) so that significant errors can be expected when calculating relative permeabilities based on assumption of a uniform saturation (Nordtvedt et al., 1994). In the dynamic method, the calculation of the derivatives of data can introduce large errors in the estimates of relative permeability values (Tao and Watson, 1984). The relative permeabilities are calculated at the exit face, so only values corresponding to saturations above the shock saturation are obtained (Buckley and Leverett, 1942). This saturation range may be very narrow, and in a strongly wetting system, only end-point values may result.

The most significant problem of both methods is that the analyses are based on very restrictive assumptions regarding the mathematical models of the experiments, assumptions which are never validated. The most serious objection is the neglect of capillary pressure (Sigmund and McCaffery, 1979; Richmond, 1988). Failure to account for capillary pressure effects in dynamic displacement experiments can lead to very large errors in the estimates, the magnitude of which is a function of the flow velocity (or capillary number) (Richmond, 1988). While some investigators have sought to eliminate capillary pressure effects by conducting dynamic displacement experiments at very high flow rates, capillary effects are persistent, and can cause significant errors even when using flow velocities well beyond that corresponding to a frequently cited scaling criterion (Rapoport and Leas, 1953). Furthermore, there is no evidence that the relative permeabilities determined under such conditions will resemble those corresponding to quasi-static displacements characteristic of reservoir flows, the conditions under which the relative permeabilities are usually desired.

The use of the conventional dynamic method in studies of relative permeabilities has likely led to a number of contradictory assessments of the effect of various process variables on relative permeability, and also certainly invalidates many experimental studies of two-phase flow. In a recent study, Chang et al. (1997) found large differences between conventional estimates obtained for dynamic experiments conducted at two different flow rates. They found some consistency between the relative permeabilities obtained from conventional steady-state analysis and the dynamic experiment conducted at the higher flow rate. They also found that the one-dimensional saturation distributions measured for the lower rate dynamic experiment were fairly consistent with those corresponding to the higher flow rate when capillary pressure effects were included in the simulation (pressure drop values were not compared). Such results are consistent with the observation that capillary pressure effects, when not taken into account in the estimation, can result in large errors in estimates of the relative permeability curves. Furthermore, it raises the question as to what differences there may actually be between "steady-state" and "unsteady-state" relative permeabilities, if accurate estimates were obtained from the experimental data.

Several studies have reported effects of flow velocity, or capillary number (ratio of viscous-to-capillary forces) on the relative permeabilities (Amaefule and Handy, 1982; Fulcher et al., 1985). Surely little useful information can be expected about the effects of capillary number on relative permeabilities calculated with the conventional analysis of dynamic data since it does not account for capillary pressure effects at all. When the experimental studies that generated relative permeabilities without reconciling capillary effects are discarded, there is little experimental information available to assess the Darcy model or functional dependencies on relative permeabilities.

Sigmund and McCaffery (1979) reported a method to estimate relative permeabilities that included capillary pressure effects. They obtained relative permeabilities by solving a parameter estimation problem, whereby they determined parameters within power-model representations of the relative permeability that minimized a sum of squared differences between measured values of pressure drop and production and the corresponding values calculated using a one-dimensional, homogeneous representation of the Darcy model (Eqs. 1–5). However, the method is not reliable because the prior assumption of the functional representations can result in inaccurate estimates (Kerig and Watson, 1986).

Watson et al. (1988) posed the problem as one of *functional* estimation, recognizing the mathematical model as an element in the estimation process that can be selected based on the experimental design, the representation of the porous media properties, and indeed, the chosen constitutive relations. They developed a generalized, regression-based method for estimating the two-phase flow functions (relative permeabilities and capillary pressure) that is directed to obtaining the most accurate estimates of the unknown functions from the available data, and is not limited by the form of the mathematical model for the experiments, the experimental design, or by which unknown functions are to be determined. Its use has been explored with a wide variety of experimental scenarios (Richmond and Watson, 1990; Nordtvedt et al., 1993, 1994; Mejia et al., 1995) and it has been extended to the estimation of three-phase flow functions (Mejia et al., 1996; Nordtvedt et al., 1996). This methodology is summarized in the following subsections.

Mathematical Model. The mathematical representation of the experiments is a critical element in any inverse method. Any assessment of quality of estimates requires that the mathematical model be the "true" model. If it is evident that the model of the experiment is not the true model, the property estimates may have little resemblance to the actual properties. Estimates obtained under such conditions, if pursued at all, should be called *apparent* properties, since they are a function of the estimation process and thus are not *intrinsic* properties. The model should basically be sufficiently complete so that all the important physical effects within the experiment are represented by that model. The assessment of the model is discussed in the "Validation" section.

The mathematical model used here is given by Eqs. 1–5, together with appropriate specifications for the boundary and initial conditions, fluid properties, and any porous media properties that are not to be estimated from the experiment. The fluid properties can be measured independently, and boundary conditions specified on the basis of the manner in which the experiment is conducted. The porous medium properties and initial fluid saturations present greater challenges.

One can assume these properties are uniform within the media and determine the average values of the properties independently, as done with the conventional estimation methods. The average porosity and permeability can be readily determined in experiments involving only a single saturating fluid phase. With the regression-based method, information about spatial variations in those properties could be included, if known. For example, one can use imaging to determine porosity and initial saturation distributions and include those within the mathematical model. Permeability distributions cannot be accurately determined. A method to estimate permeability distributions from CT data has been reported (Withjack et al., 1991). However, it is based on the representation of the porous media as a bundle of uniform tubes, so the reliability of the estimates is doubtful. While we do anticipate further developments in the ability of imaging methods to provide reliable estimates of permeability distributions, we now take the permeability to be uniform and provided by the measured average value. Future studies could incorporate the estimates of permeability within the analysis when they are available (Mejia et al., 1995). For our experiments, we have chosen samples that appear to be relatively uniform.

As mentioned previously, any spatial variations in the saturation-dependent relative permeability functions are presumed to be much less than the absolute permeability. Zonal representations for these properties could be used and may be useful for experiments for which there are distinct changes in the properties, such as experiments on composite cores (Mejia et al., 1995). Here we assume that these flow functions are uniform within the medium (as done with conventional methods).

The capillary pressure could be measured independently (Nordtvedt and Kolltveit, 1991; Leverett, 1941) and included in the mathematical model for the laboratory experiment. However, due to potential difficulties in replicating initial conditions and the inordinate length of experimental times required, it is most desirable to determine the capillary pressure and relative permeabilities simultaneously from the same experiment.

Functional Representations. Since ultimately a finite set of data is collected, the unknown functions must be represented with a finite number of parameters. While we expect the properties to be smooth functions of saturation, the actual form of the functions is not known. We use B-splines to represent the properties, since they can represent any smooth function arbitrarily accurately (Schumaker, 1981). At the same time, they have many convenient computational features.

B-splines are locally supported basis functions (they have the value zero beyond their region of support), the local support being defined by the knot locations. Each basis function is defined over $m+1$ knots, where m is the order of the spline, and can be represented by a polynomial of the selected order. The extended partition is specified by the number and locations of k interior knots along with m knots at either end of the domain. With a basis function belonging to each set of $m+1$ contiguous knots, there will be $m+k$ basis functions. For a selected partition, the spline function is specified by the $m+k$ coefficients, each of which corresponds to a basis function.

The property representations are given by

$$k_{ri}(s_i) = \sum_{j=1}^{N_i} C_j^i B_j^m(s_i, \vec{y}^i), \quad i = 1,2 \tag{6}$$

$$p_c(s_i) = \sum_{j=1}^{N_c} C_j^c B_j^m(s_i, \vec{y}^c). \tag{7}$$

where $\vec{y}$ is the extended partition, B_j^m is the jth B-spline, and C_j is the corresponding coefficient. We select the extended partition and the coefficients through solution of a sequence of parameter estimation problems, as discussed in the following subsection.

Parameter Estimation. For a given B-spline representation (i.e., order m and extended partition $\vec{y}$), the properties are specified by the coefficient vector:

$$\vec{\beta} = \left[C_1^1, \ldots, C_{N_1}^1, C_1^2, \ldots, C_{N_2}^2, C_1^c, \ldots, C_{N_c}^c\right]^T. \tag{8}$$

Values for the coefficients are determined through solution of the parameter estimation problem represented by

$$\text{minimize} \quad J(\vec{\beta}) = \left[\vec{Y}_{\text{meas}} - \vec{Y}_{\text{sim}}(\vec{\beta})\right]^T \mathbf{W} \left[\vec{Y}_{\text{meas}} - \vec{Y}_{\text{sim}}(\vec{\beta})\right] \tag{9}$$

subject to the constraints

$$\mathbf{G}\vec{\beta} \geq \vec{\beta}_{\text{con}}. \tag{10}$$

$\vec{Y}_{\text{meas}}$ is the vector containing measured data. A variety of data can be used, including pressure drop, production, and saturations measured within the sample. $\vec{Y}_{\text{sim}}(\vec{\beta})$ is the vector containing the corresponding values calculated by numerical simulation of the displacement process using the mathematical model of the displacement experiment. $\mathbf{G}$ is the matrix specifying the linear inequality constraints on the parameters to ensure monotonicity of the properties and nonnegativity for the relative permeabilities throughout the estimation process (Watson et al., 1988), and $\mathbf{W}$ is the weighting matrix chosen for maximum likelihood estimates of the parameters (Watson et al., 1990). A trust-region based, linear-inequality constrained, Levenberg-Marquardt algorithm is used to solve the parameter estimation problem.

Suitable knot partitions are to be selected for the B-splines. Several different methods have been used to select the partitions in different experimental situations (Richmond and Watson, 1990; Nordtvedt et al., 1993), but the basic principles are the same. The goal is to eliminate significant bias errors,

while limiting unnecessary variance errors (Watson et al., 1988; Kerig and Watson, 1986). This is accomplished by successively increasing the number of knots (and hence also increasing both the number of unknown parameters and the candidate solution space for the unknown functions) until the measured data have been adequately described through simulation with the mathematical model and property estimates. This can be assessed through examination of residuals (Richmond and Watson, 1990; Watson et al., 1990), which are differences between the measured and calculated quantities. Knots can be added to those regions of the properties that appear to be responsible for the greatest discrepancies between the measured and predicted data. One can also monitor successive reductions in the performance index as knots are added, and use as estimates those values corresponding to the point at which significant reductions in the performance index cannot be obtained with modest increases in the number of parameters (Watson et al., 1988).

Validation

Regardless of the methodology used to estimate the relative permeabilities, the estimates should be validated. A minimal validation is to use the estimates together with the mathematical model of the experiment to simulate the experiment. If the simulation provides a reasonably accurate calculation of the measured values, the elements of the estimation process, that is, the mathematical model and the estimates of the properties, are validated. This does not prove the results are correct, since there may be other sets of properties that could also provide accurate simulations. Still, it certainly provides a measure of confidence. An unsatisfactory match means that one of the elements of the estimation has failed, so the validity of the estimates must be questioned.

Other, and more stringent, validations can be devised. For example, one could evaluate assumptions of the mathematical model by using the more complete model for simulation, if those neglected physical effects can be estimated. The mathematical model can be further tested by comparing predictions of measured fluid states with measurements that were not included in the estimation.

The mathematical model of the experiment should be sufficiently accurate so that the differences between the observed and "true" values can be attributed to random errors. This is a most stringent test, but it is indeed what is necessary for an experimental demonstration of Darcy's Law. This condition can be assessed with a residual analysis. The residuals —differences between measured and calculated values— should approach the level of the magnitude of the errors expected with the measurement devices. Ideally, one would like a plot of the residuals with the calculated values to appear random, with a fairly uniform distribution (Draper and Smith, 1981). Achieving this level of validation may require some careful examination, perhaps including effects due to the model being nonlinear in the parameters (Cook and Tsai, 1985) and modeling of the measurement process, and certainly requires careful attention to all the elements of the estimation process.

To what extent have property estimates and mathematical models been validated? Estimates obtained using the regression-based method (Watson et al., 1988) have been successfully validated through fairly precise simulation of experimental data in several cases (Richmond and Watson, 1990; Nordtvedt et al., 1993, 1994). We are not aware of any successful validations of conventional estimation methods. If capillary effects are included in the simulations with relative permeabilities obtained using conventional methods that neglect capillary effects, we expect that very few successful validations would be obtained. On the other hand, there have been a number of publications where differences between simulated experiments and measured data greatly exceed the accuracy with which the measurements are made. In many cases, we believe these failures can be attributed to the estimation method used and thus do not provide for a real assessment of the mathematical model.

The successful experimental validations have been based on data collected outside of the sample. Conventional experiments, for which a constant injection rate and only data measured outside of the sample are used, may not provide estimates of the multiphase flow functions that are as accurate as one may desire. That is, the estimates may be consistent with the measured data, but if there is insufficient "information content" in those data, other estimates of the functions may also reconcile the data. This is discussed later in the Experimental Results and Discussion section. In such cases, it is likely that, while a number of different estimates may reconcile the data collected outside of the sample, those estimates may provide different predictions of fluid states within the sample. If such observations of the fluid states were available, more accurate estimates of the functions could be expected consistent with having further constraints on the estimates of the properties. Reconciliation of such data also provides for a substantially more stringent test of the assumptions made in the analysis of the data.

Two previous applications using measured saturation values to estimate properties have been reported (Mejia et al., 1995; Chardaire-Riviere et al., 1992). However, neither study reported very good agreement between measured and predicted values and therefore failed to validate the estimate process. Chardaire-Riviere et al. used power law and piecewise linear functional representations of the relative permeabilities in their estimation method, which may result in significant estimation errors (Kerig and Watson, 1987; Kerig and Watson, 1986). The experimental situations studied by Mejia et al. were rather complicated, with significant sample heterogeneity and perhaps unstable flows. Successful validations of fluid states within the media, together with conventional measurements outside the sample, are necessary to provide experimental validations of the Darcy model.

Assessment of Experimental Design

Since saturation information is not easily obtained, it is desirable to assess whether such additional measurements will significantly improve the accuracy of estimates of the properties. This is best done using hypothetical (simulated) experiments. The accuracy with which the properties may be estimated for a given experimental scenario can be evaluated with a linearized covariance analysis (Kerig and Watson, 1987), as summarized in the Appendix. In this section we evaluate the improvements that may be attained in the accuracy of estimates when saturation profile measurements are included in

addition to the conventional measurements of pressure drop and production.

The analysis is carried out by specifying the experimental design (the manner in which the experiment is conducted, the measurements to be taken and their accuracy) and the sample properties. The experimental design associated with the saturation measurements is based on the use of MRI (Chen et al., 1993, 1994; Kulkarni and Watson, 1997). MRI provides some significant advantages over the other techniques that have been used to monitor saturation. The entire sample is imaged, thus allowing for verification of material balances. The submillimeter resolution that is available provides for an essentially continuous representation of the saturation distribution. MRI can also be used to determine the porosity distribution.

Two different experimental scenarios are considered. In the first, the conventional constant injection rate experiment is used. In the second, we use multiple rates. In both scenarios, the experimental process is taken to be primary drainage, for which oil (denoted as phase 1) is to be injected into a sample initially fully saturated with the aqueous phase. A constant pressure is maintained at the outlet end. We take the properties to be uniform and neglect gravity so that only a single spatial dimension need be used in the mathematical model. With these simplifications to Eqs. 1 and 2, and after eliminating the velocities, the model, together with initial and boundary conditions, is

$$\frac{\partial}{\partial t}(\phi\rho_1 s_1) = \frac{\partial}{\partial z}\left(\frac{Kk_{r1}\rho_1}{\mu_1}\frac{\partial p_1}{\partial z}\right) \tag{11}$$

$$\frac{\partial}{\partial t}(\phi\rho_2 s_2) = \frac{\partial}{\partial z}\left(\frac{Kk_{r2}\rho_2}{\mu_2}\frac{\partial p_2}{\partial z}\right) \tag{12}$$

where the fluid saturation and pressures are related as follows

$$p_1 - p_2 = p_{c12} \tag{13}$$

$$s_1 + s_2 = 1. \tag{14}$$

The initial conditions are

$$s_1(z) = 1 \tag{15}$$

$$p_1(z) = p_{\text{out}}$$

where p_{out} is the pressure maintained at the outlet end.

The boundary conditions at the inlet, $z = 0$, are

$$-Kk_{r1}\frac{\partial p_1}{\partial z} = q_{1\text{in}} \tag{16}$$

$$\frac{\partial p_2}{\partial z} = 0$$

where $q_{1\text{in}}$ is the injection rate of fluid phase 1.

The boundary conditions at the outlet, $z = L$, are

$$\begin{aligned}
&\text{if} \quad p_{c12}(L) > 0, \quad && p_1 = p_{\text{out}} \\
& && \frac{\partial p_1}{\partial z} = 0 \\
&\text{if} \quad p_{c12}(L) < 0, \quad && \frac{\partial p_2}{\partial z} = 0 \\
& && p_2 = p_{\text{out}} \\
&\text{if} \quad p_{c12}(L) = 0, \quad && p_1 = p_2 \\
& && p_2 = p_{\text{out}}
\end{aligned} \tag{17}$$

The boundary conditions implement the capillary end-effect discussed in Dullien (1992). The boundary conditions require that the phase pressures be continuous across the outlet face. This means that both fluid phases will flow across the outlet face only when the capillary pressure just outside the outlet face of the core sample (taken here to be zero) and at the outlet face of the core sample are equal. If the capillary pressures are unequal, only the non-wetting phase (the phase with the higher pressure) is able to flow across the outlet face.

A fully implicit finite-difference method is used to calculate pressures and saturations. The relative permeability and capillary pressure functions used are those specified as "true" in Figures 1–3, and other information associated with the specified properties, experiment, and simulation are tabulated in Table 1.

In the first experimental scenario, a single injection rate is used with a flow velocity comparable to those typically encountered in underground reservoirs. In the second experimental scenario, a set of three constant rates are used, starting with the injection rate in the low-rate case, and then increasing successively. The values corresponding to measured quantities calculated with the "true" properties are shown in Figures 4–6. The variances of measurement errors in production, pressure drop, and saturation data in the single-rate experiment were taken to be 0.06 cm^3, 1 kPa, and 0.004, respectively. In the multirate experiment they were taken to be the same, except for the last rate step, where they were taken as 0.15 cm^3, 5 kPa, and 0.01, respectively, to reflect the ex-

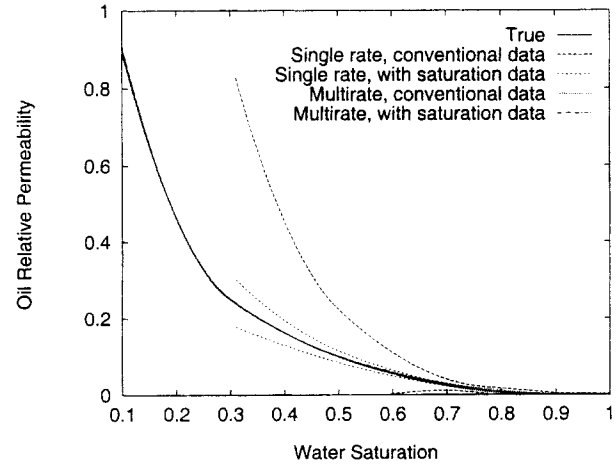

Figure 1. Oil-relative permeability and 95% confidence intervals for different experimental designs.

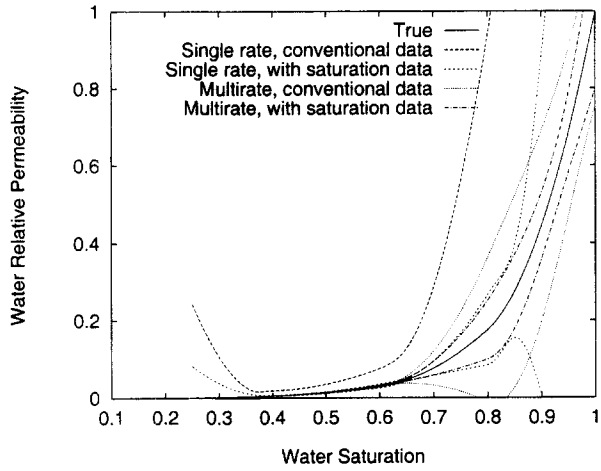

Figure 2. Water-relative permeability and 95% confidence intervals for different experimental designs.

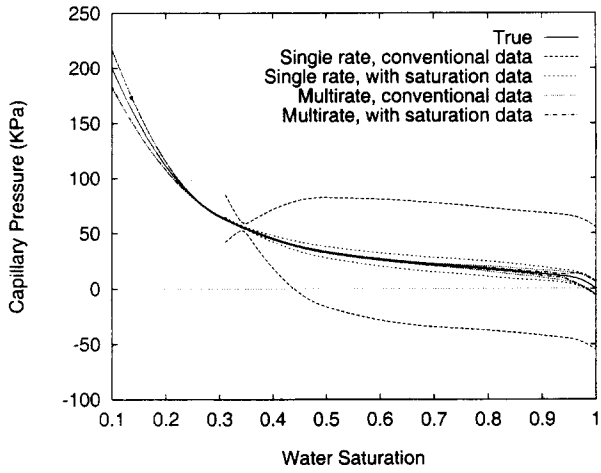

Figure 3. Capillary pressure and 95% confidence intervals for different experimental designs.

pected increase in the errors with the larger values to be measured.

The results of the covariance analysis are shown in Figures 1–3, where 95% confidence intervals for the estimated flow functions are shown for the two scenarios with and without saturation data. The conventional data include measure-

Table 1. Simulation Details of Experiments Used in Covariance Analysis

Water viscosity (cp)	1.0
Oil viscosity (cp)	1.5
Core length (cm)	10.0
Core diameter (cm)	3.5
Porosity (%)	30.0
Absolute permeability (mD)	50.0
Initial water saturation	1.0
Injection rates (cm^3/min)	
Water	0.0
Oil (low rate case)	0.1
(multirate case)	0.1, 0.5, 5.0

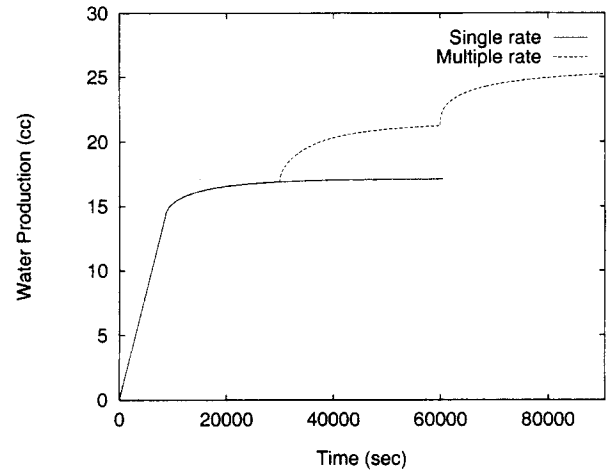

Figure 4. Water production data for the two experimental designs used in the linearized covariance analysis.

ments of production and pressure drop only. It should be noted that a water saturation of about 0.3 is reached at the end of the hypothetical single-rate experiment. The measured data, therefore, contain information about the flow function only over a range of water saturation from 0.3–1.0. The confidence intervals for the single-rate experiments are finite only over that range. For the multirate hypothetical experiment, however, a lower water saturation is achieved and the confidence intervals are finite over a wider range of water saturation.

Compared to the single-rate experimental case, more accurate estimates can be obtained by including saturation measurements or using multiple rates. The saturation data represent additional information, so an improvement in the accuracy is certainly expected. The large improvement obtained in the accuracy of estimates by using multiple injection rates with just conventional data is somewhat surprising. One advantage of the multiple rates is that a greater range of saturation is accessed in the experiment, thus providing additional

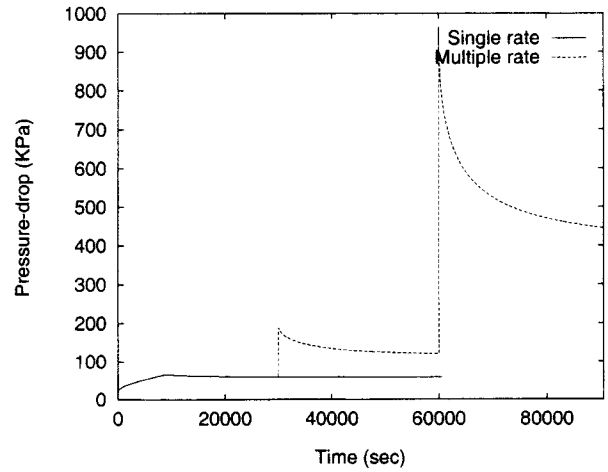

Figure 5. Pressure drop data for the two experimental designs used in the linearized covariance analysis.

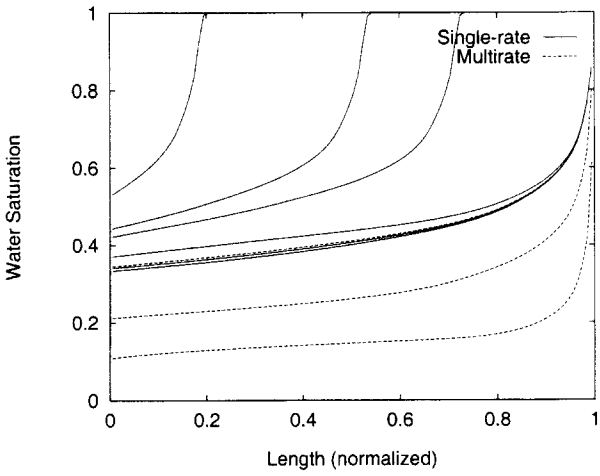

Figure 6. Water saturation profile data for the two experimental designs used in the linearized covariance analysis.

In the single rate experiment, water saturation profiles are measured at 20, 70, 100, 250, 550 and 950 min, respectively. In the multirate experiment, they are additionally measured at 1450 min.

information about the flow functions over a greater range. We expect that the changes in flow rates also increase the information content of the data by allowing the system to be observed under different levels of viscous-to-capillary forces. Certainly, the use of multiple injection rates is a very cost-effective method for improving the accuracy of the estimates.

The best accuracy is obtained with the inclusion of saturation data while using multiple injection rates. Most notably, the saturation data serve to improve the accuracy with which the wetting-phase relative permeabilities can be estimated (Figure 2).

It should be emphasized that the confidence intervals are based on a linearized covariance analysis and must be considered approximate. In particular, when they are large, little meaning should be attached to their shape. While the actual accuracy of the confidence intervals may not be great, they are most useful to evaluate experimental designs by comparison, as done here, or for indicating which regions of the properties might be relatively more accurately determined. The meaning of pinch-off points, which sometimes occur close to the lowest saturation values represented by the hypothetical experiments, is not entirely clear. We did not find such pinch-off points to correlate in any way with knot locations and believe them to be an artifact caused by the explosion of the confidence interval beyond the saturations encountered in the experiment.

Experimental Results and Discussion

In this section, the estimation of flow functions from actual experiments using the two experimental scenarios presented in the previous section is demonstrated. Two-phase dynamic displacement experiments were conducted on Texas Cream limestone samples. Cylindrical samples were laterally sealed using epoxy (Stycast 2651) and mounted in plexiglass coreholders with O-rings to conduct the displacement experiments. The apparatus is shown in Figure 7. All MRI measurements were conducted with a GE 2-Tesla CSI-II imager/spectrometer with a 31-cm magnet bore and equipped with a 20 G/cm shielded gradient coil and a birdcage RF coil. Either hexadecane or dodecane was used as the oleic phase and deuterium oxide (D_2O) was used as the aqueous phase. Protons are imaged, so only the oil phase is observed. A known quantity of distilled water was used as a reference sample for signal intensity calibration purposes (Chen et al., 1993, 1994).

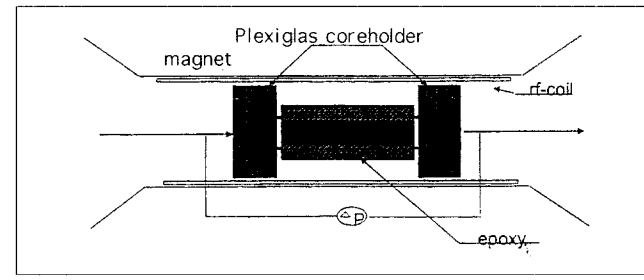

Figure 7. Experimental setup for conducting displacement experiments and NMR imaging.

The experiments analyzed in this study are drainage experiments, for which the sample is initially completely saturated with the aqueous phase. An image of the sample completely saturated with the observed fluid phase is desired for determining saturation. Since the fluid in the initial state (D_2O) is not being observed, the sample was initially completely saturated with pure water and an image taken. Then, the sample was dried, resaturated with D_2O and the drainage experiments conducted by injecting oil. Oil saturation can then be calculated by material balance for the proton species (Chen et al., 1993, 1994; Kulkarni and Watson, 1997).

Single-rate experiment

In the first experiment, oil was injected at a constant flow rate into a sample completely saturated with the aqueous phase and the pressure-drop and oil saturation profiles were measured until the steady state was attained. Hexadecane was used as the oleic phase and D_2O was used as the aqueous phase. Water production was estimated using integrals of the oil saturation profiles with material balances. The sample and fluid properties and experimental conditions are shown in Table 2.

The rock sample used in this work appears to be quite homogeneous, as indicated by the porosity profile shown in Fig-

Table 2. Core and Fluid Properties for the Single-Rate Primary Drainage Experiment

Water viscosity (cp)	1.26
Oil viscosity (cp)	3.34
Core length (cm)	4.9
Core diameter (cm)	2.5
Porosity (%)	26.6
Absolute permeability (mD)	10.2
Initial water saturation	1.0
Injection rates (cm^3/min)	
Water	0.0
Oil	0.05

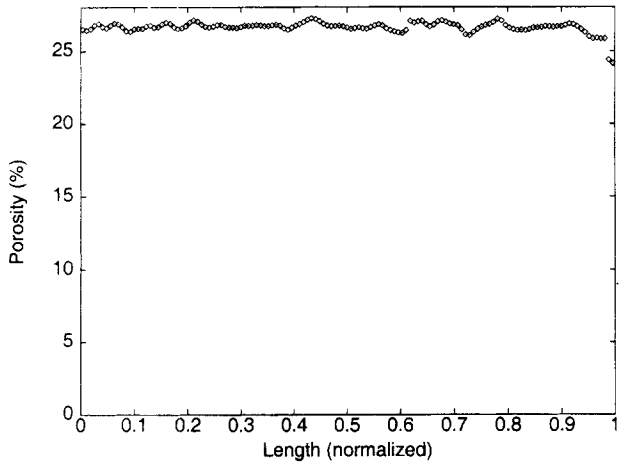

Figure 8. Porosity profile for sample used in single-rate primary drainage experiment.

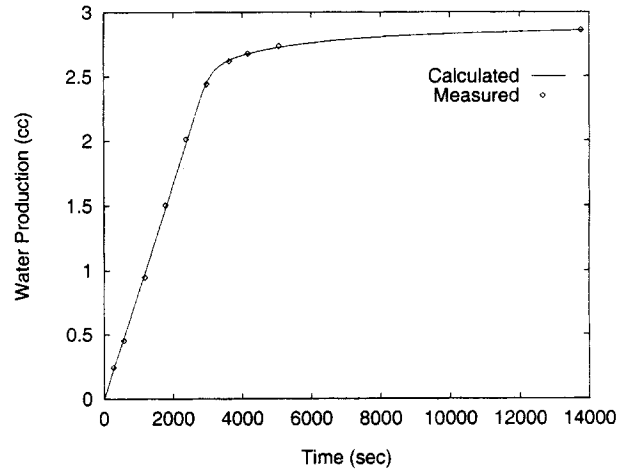

Figure 9. Calculated and measured water production data in single-rate primary drainage experiment.

ure 8. The same mathematical model discussed previously (see Eqs. 11–17) was used. The absolute permeability was taken to be uniform. The porosity variation was accounted for by assigning each grid block the average value of porosity observed over the block. Multidimensional simulation was used to confirm that gravity segregation is not significant and that one-dimensional simulation of flow is adequate.

The pressure drop, saturation profile, and water production data were used in the regression-based approach to estimate the relative permeability and capillary pressure functions. The production data were not measured independently, but were calculated with a material balance using integrated saturation distributions. Although it is not necessary to include the production in the performance index, since it does not represent independent information, it seemed to assist in attaining the global minimum. Starting with just one knot for the B-spline representation of each flow function, successive parameter estimation problems were solved with increasing numbers of knots. It was found that the performance index did not significantly decrease when more knots were added beyond representations with seven interior knots each for the relative permeability and six interior knots for the capillary pressure representation. These representations were chosen as the final estimates. A total of 29 parameters were estimated in the final step of the regression-based approach.

The measured pressure drop, saturation, and water production, along with values calculated using the mathematical model of the experiment with the properties estimates, are shown in Figures 9–11. The estimated flow functions, along with 95% confidence intervals, are shown in Figures 12 and 13. An assumption in computing the confidence intervals is that the model is the "true" model which, as discussed in the "Validation" section, may not so easily be established. The confidence intervals are useful here as indications of the relative degree of information that is available from the data for estimating different regions of the properties. From Figure 11, it is apparent that a water saturation of 0.4 is reached at the end of the experiment. Consequently the flow functions cannot be reliably estimated for water saturations below that value. The agreement between estimated and measured production and pressure drop data is quite good. The largest deviations in the calculated and measured pressure-drop values occur before breakthrough. This could be indicative of some variations in the permeability distributions (Watson et al., 1985). The estimated saturation profiles agree quite well with the measured saturation, except for the saturations near the inlet face corresponding to the last saturation profile (229 min). Note that there is little information about the properties corresponding to saturation values less than 0.5 anyway since there are relatively few data with saturations in that range.

Clearly, the saturation data are not reproduced as precisely as the pressure drop and production. There are several reasons for this. Saturation is not measured as accurately as the pressure. We anticipate that the saturations are accurate to about 5%, while the pressure may be accurate to 1%. This relative accuracy is reflected in the weights used in the performance index. Reconciliation of saturation, however, is much more challenging because it represents point informa-

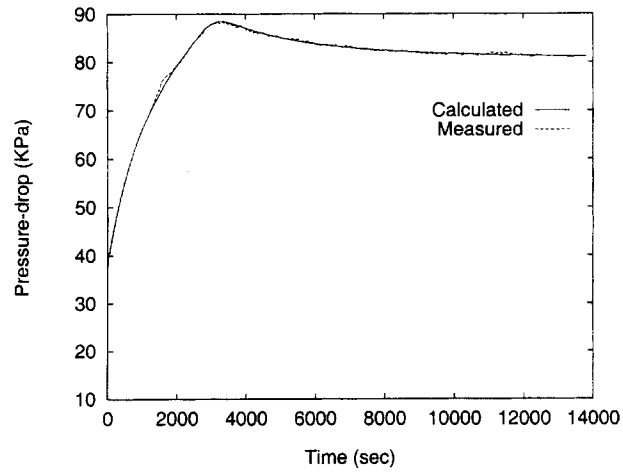

Figure 10. Calculated and measured pressure-drop data in single-rate primary drainage experiment.

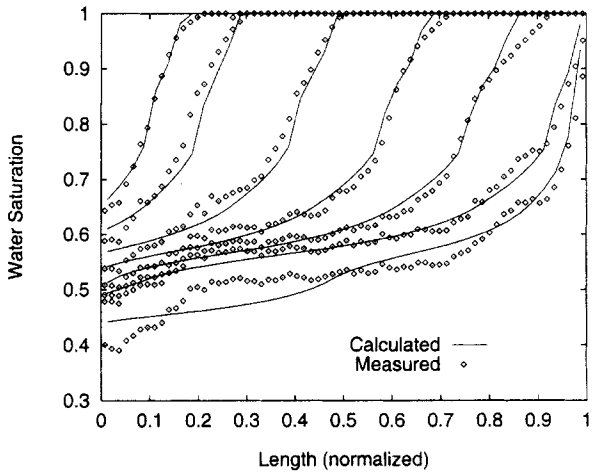

Figure 11. Calculated and measured water saturation profiles for single-rate primary drainage experiment.

Starting from the upper left, profiles correspond to times 4, 9, 19, 29, 39, 49, and 229 min.

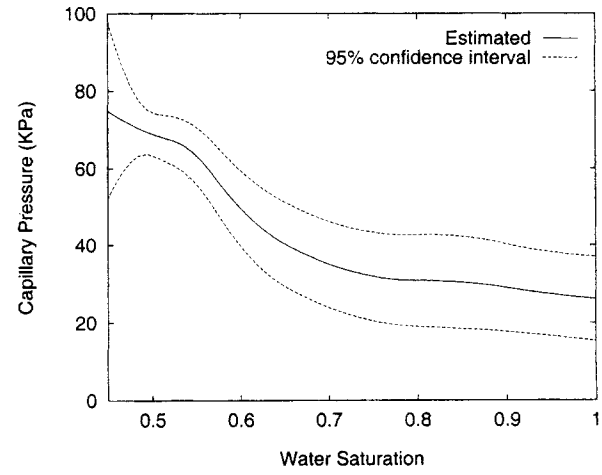

Figure 13. Estimated capillary pressure and 95% confidence interval for single-rate primary drainage experiment.

tion, whereas the pressure drop and production (the only data used in conventional experiments) represent integrated information. With integrated data, the local variations tend to be averaged. Another issue is that variations in the porosity (except for axial variations) and permeability are not taken into account. These variations may cause deviations in saturation that are not resolved with the current model of the experiment.

Figures 12 and 13 show that the confidence intervals for the estimated functions are relatively broad, indicating that the single-rate experimental design does not appear to be sufficient for accurate determination of the flow functions. The interplay between imposed constraints (monotonic increasing and $k_{rw}(1) = 1.0$) and relatively low information content (indicated by the large confidence intervals) may be responsible for the unusual shape of the water relative permeability curve. Given the large confidence intervals, there may be other curves, more conventional in appearance, that could also reconcile the data. The estimated flow functions do reconcile all the data reasonably well, indicating that the property estimates are consistent with the measured data. The widths of the confidence intervals in this case are larger than those shown in *Assessment of Experimental Design* due to the lesser accuracy assumed for the pressure measurements and sparser production and pressure drop data.

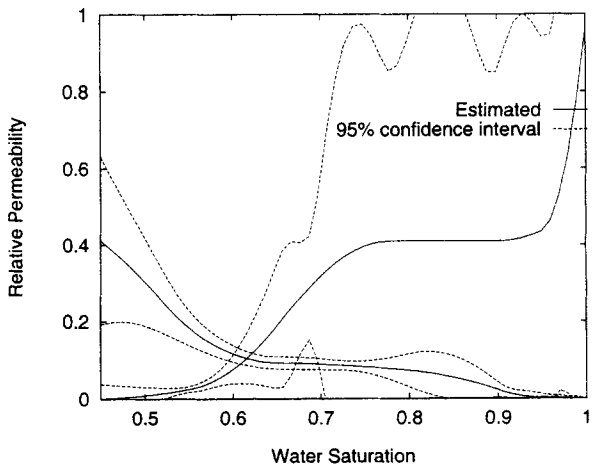

Figure 12. Estimated relative permeability and 95% confidence interval for single-rate primary drainage experiment.

Multirate experiment

A multirate primary drainage experiment was performed on a second Texas Cream limestone sample. Dodecane was used as the oleic phase and D_2O was used as the aqueous phase. Pressure-drop and oil saturation profiles were monitored during the displacement. The water production data were computed by integrating the oil saturation profiles and material balance about the initial state. Starting with a small oil injection rate, the oil injection rate was incremented in two steps. A water saturation of 0.16 was observed at the end of the last rate step. The details of the sample and fluid properties used in the experiment are provided in Table 3. The porosity profile for the rock sample is shown in Figure 14. As for the single-rate case, the simulations account for the porosity heterogeneity by assigning each grid block a distinct porosity calculated from the porosity profile.

The analysis was conducted somewhat differently than the previous experiment so that we could further evaluate the

Table 3. Core and Fluid Properties for the Multirate Primary Drainage Experiment

Water viscosity (cP)	1.26
Oil viscosity (cP)	2.08
Core length (cm)	3.86
Core diameter (cm)	2.5
Porosity (%)	24.08
Absolute permeability (mD)	25.74
Initial water saturation	1.0
Injection rates (cm^3/hr)	
Water	0.0
Oil	0.06, 0.33, 2.0

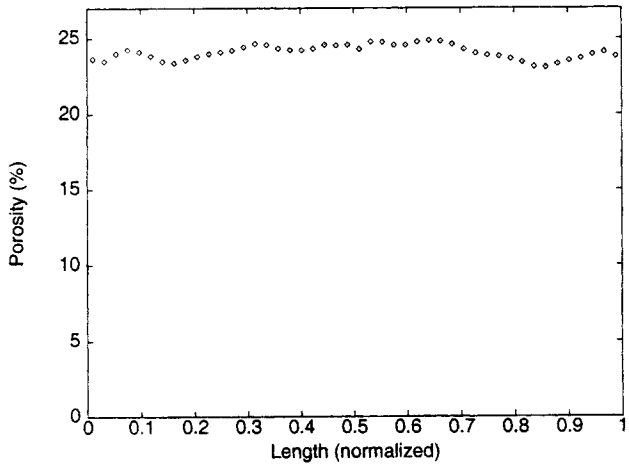

Figure 14. Porosity profile for sample used in multirate primary drainage experiment.

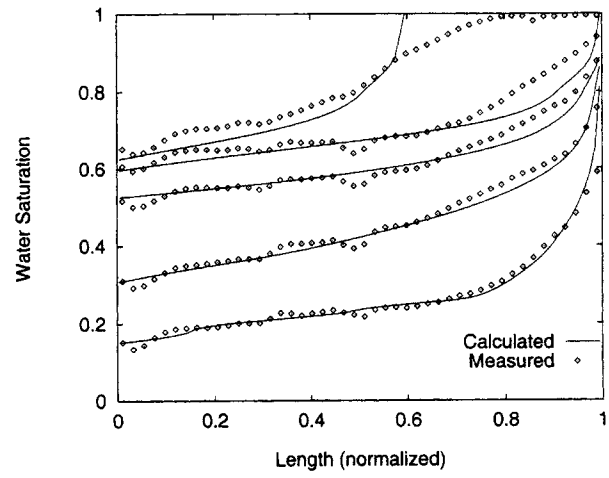

Figure 16. Calculated and measured water saturation profiles for multirate primary drainage experiment.

Starting from the upper left, profiles correspond to times 12, 22, 238, 500 and 696 min.

model of the experiment. The calculated production and several saturation profiles were not used in the estimation so that predictions of the model could be tested. Starting with a single knot in each representation, it was found that the performance index did not decrease significantly beyond a representation with seven interior knots in the water relative permeability representation, eight interior knots in the oil relative permeability representation, and 10 interior knots in the capillary pressure representation. A total of 32 parameters were estimated in this final step of the regression-based approach.

The measured pressure drop and saturation, and values calculated using the estimated properties, are shown in Figures 15 and 16. The estimated flow functions and the 95% confidence intervals are shown in Figures 17 and 18. Note how estimates are obtained over a much broader range than for the single-rate experiment. The confidence intervals indicate that the oil relative permeability and capillary pressure are accurately estimated over the entire range of saturation accessed in the experiment, as is the water relative permeability for the majority of the saturation range.

Again, there is excellent agreement between calculated and measured pressure-drop values. For the most part, the saturation data are reconciled reasonably well. The dip in the saturation values in the center of the sample is an artifact of the analysis of NMR data.

The saturations greater than $S_w = 0.9$ in the first profile were not so well reconciled. A similar feature was seen in one of the profiles in the first experiment (see the profile corresponding to 39 min in Figure 11). This may be due to the relatively low density of data in that region. The saturation profile corresponding to 22 min is not accurately reconciled in the vicinity of the outlet of the sample. Close inspection shows that the differences between measured and calculated values right next to the outlet for the last two profiles are relatively large, and for all the profiles after breakthrough, the measured saturation distributions are not as steep as the calculated distributions. The standard boundary

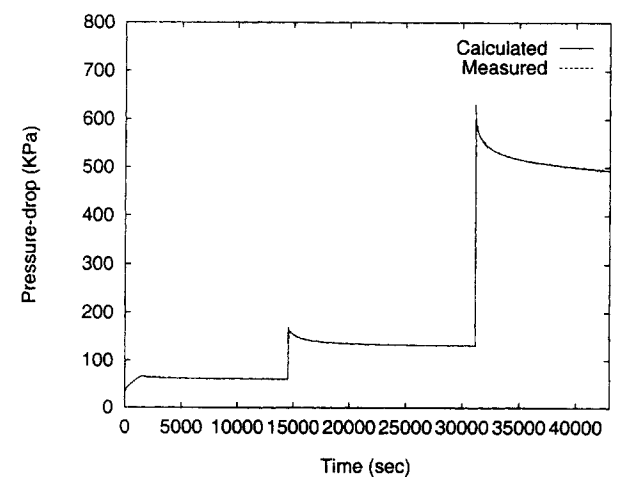

Figure 15. Calculated and measured pressure-drop data in multirate primary drainage experiment.

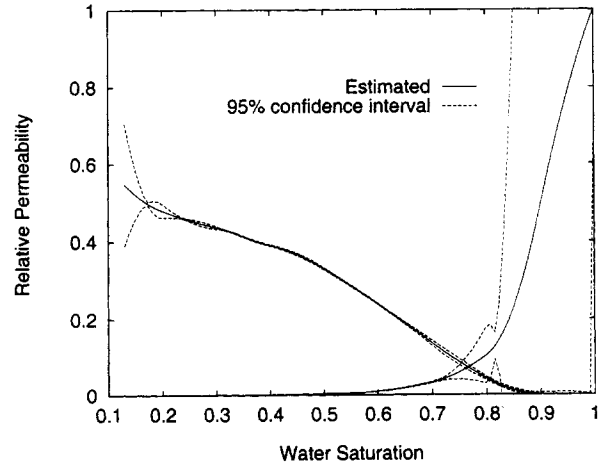

Figure 17. Estimated relative permeability functions and 95% confidence intervals for multirate drainage experiments.

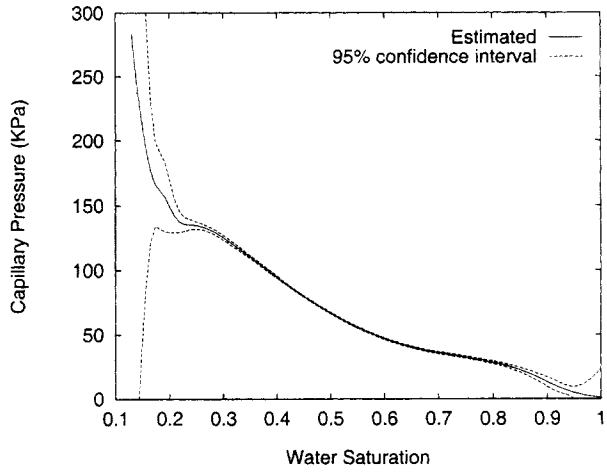

Figure 18. Estimated capillary pressure and 95% confidence interval for multirate primary drainage experiment.

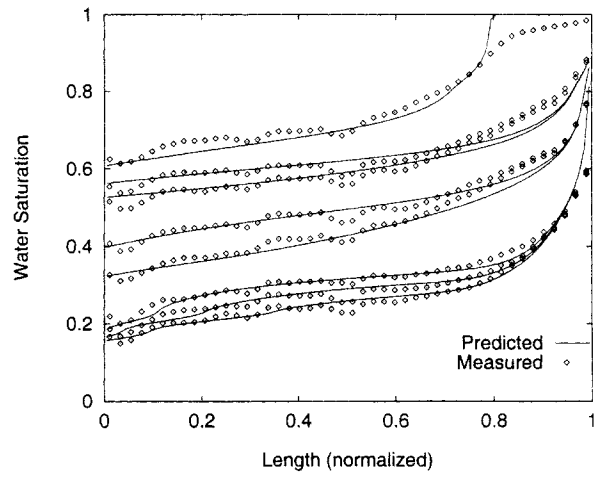

Figure 20. Predicted and measured saturation data in multirate primary drainage experiment.

Starting from the upper left profiles correspond to times 17, 46, 168, 280, 421, 562, 596, and 647 min.

conditions call for the saturation at the outlet to remain at the value corresponding to zero capillary pressure even after breakthrough of the injected fluid. The saturation that might correspond to the outlet face appears to be decreasing with time. The reason for the discrepancy may be due to a buildup of the displacing phase in the small gap (less than 0.5 mm) between the plexiglass end plate and the core sample endface causing a nonzero capillary just outside the core sample endface. The amount of buildup will change with time, causing the capillary pressure just outside the core sample endface to change with time, which is not represented in the model.

Consider now the prediction of saturation data and production, which were not used as part of the estimation process. The measured production, which was calculated with a material balance and integrated saturation distributions, is shown with production calculated with the model and property estimates in Figure 19. The agreement indicates that the averages of the saturation distributions are indeed accurately determined. The predictions of the saturation profiles are shown together with saturation measurements in Figure 20. The predictions describe the shape of the measured distributions, and their changes with time, quite well. The regions that are not accurately predicted—the values of saturation greater than $S_w = 0.9$ and the saturation values near the outlet—are the same regions that had the largest deviations between the measured and calculated values (see Figure 16).

Figures 21 shows the plot of scaled residuals versus scaled calculated values. The scaled values are obtained using the relation $u_{\text{scaled}} = u/\gamma_u$, where u is the calculated value and γ_u is the estimated standard deviation of the error in measurements of u. If γ_u were the true value of the standard deviation, measurement errors corresponding to the scaled values would be identically distributed (assuming independent, random errors). The pressure residuals fall into three groups, which correspond to the different rates. The values corresponding to the largest pressures seem to be randomly distributed, with no clear pattern. Patterns are observed for the

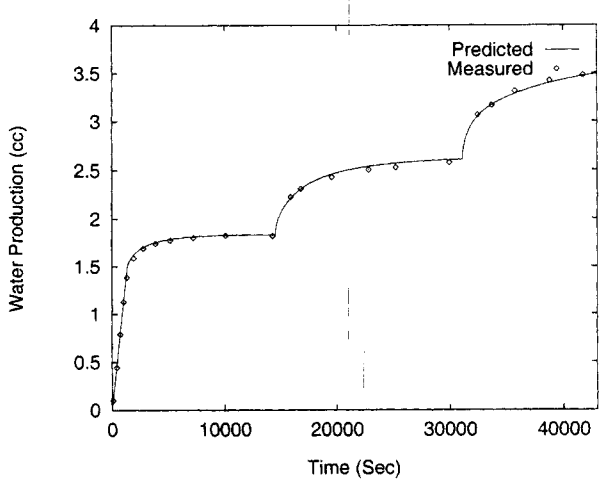

Figure 19. Predicted and measured water production data in multirate primary drainage experiment.

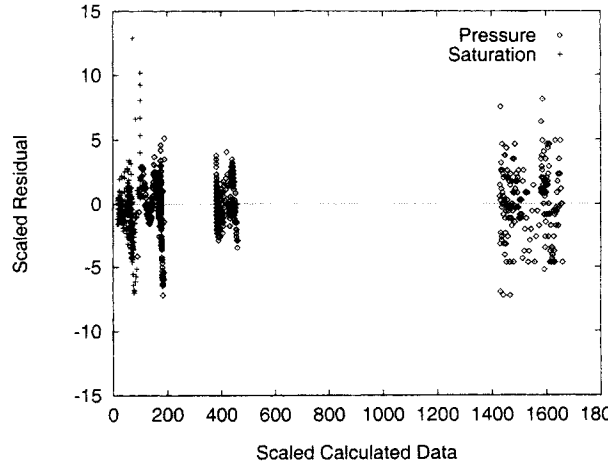

Figure 21. Residual plot corresponding to final estimates.

lower pressure and the saturations. The largest residual corresponds to the very first pressure measurement, and several of the larger saturation residuals correspond to locations next to the outlet face of the sample. For the most part, the magnitudes are reasonable.

The patterns observed in the residuals suggest that not all the assumptions of the analysis have been met. Several possible reasons for this have been discussed, most notably a possible deficiency in the boundary condition, and variations in the absolute permeability distributions. Such patterns could also be the result of assumptions of the measurement errors (here, that the error for each type of measurement is independent and identically distributed) not holding.

The analyses of the two experiments provide a measure of validation for the Darcy equation. For the first time, we find that there are estimates of the properties that provide for simulation of measured values that meet or approach the level of accuracy with which the saturation distributions and pressure drops can be measured. Further improvements in the accuracy of the estimates, and more critical assessments of the mathematical model, can be made when methods are devised for reliable determination of the permeability distribution, and a greater consistency is obtained between the laboratory experiment and outlet boundary conditions. Further analysis and modeling of the measurement processes are also desired for the purposes of statistical testing. In order to generate reliable databases from which to improve our understanding of multiphase flow, every estimate of multiphase flow properties should be carefully assessed and validated, as has been done here.

Summary

The experimental design and analysis of two-phase dynamic displacement experiments were investigated. Conventional methods for obtaining relative permeabilities from two-phase experiments may not provide reliable estimates due to failure to account for capillary effects in the experiment. Experimental designs that include either saturation profile measurements or multiple fluid-injection rates can provide substantially more accurate estimates of relative permeability than conventional experimental methods and analyses. When used together, accurate estimates of relative permeability and capillary pressure functions can be obtained over broad ranges of fluid saturations.

Methodology for validating experiments was presented and demonstrated. Validation is a necessary element for obtaining reliable estimates of relative permeability functions.

Saturation distributions and pressure drop measurements obtained in the laboratory were successfully reconciled with simulations of the experiment to a level approaching the accuracy of the measurements. Calculated predictions of production and saturation distributions were consistent with measured values of production and saturation that were not used in the estimation values. These exercises provide an experimental validation of the Darcy model for two-phase flow that has not previously been achieved.

Acknowledgment

Sang-Joon Lee provided helpful input for the statistical analyses. Support from the following sources is gratefully acknowledged: Collaborative Program for Studies of Multiphase Processes in Porous Media, sponsored by Saga Petroleum a.s. and Agip S.p.A., University-Industry Cooperative Research Program for Petrophysical and Reservoir Engineering Applications of NMR at Texas A&M University, and the Strategic Program for Advancing System and Parameter Identification, sponsored by Norges Forskningsråd.

Notation

B = B-spline basis function
D = sensitivity matrix of flow functions
$\vec{g}$ = gravity
J = objective function
k_r = relative permeability
N = number of parameters
$\boldsymbol{P}$ = covariance matrix of parameters
t = time
$\vec{v}$ = filtration velocity
$\boldsymbol{V}$ = covariance matrix of flow functions
$\vec{\beta}$ = parameter vector
$\vec{\beta}_{\text{con}}$ = constraint vector
μ = viscosity
ϕ = porosity
ρ = density
x = covariance matrix of measurement errors

Subscripts and superscripts

c = capillary
nw = nonwetting
r = relative
T = transposed
w = wetting

Literature Cited

Amaefule, J., and L. Handy, "The Effect of Interfacial Tensions on Relative Oil/Water Permeabilities of Consolidated Porous Media," *Soc. of Pet. Engs. J.*, **22**, 371 (1982).

Archer, J., and S. Wong, "Use of a Reservoir Simulator to Interpret Laboratory Waterflood Data," *Soc. of Pet. Engs. J.*, **163**, 343 (1973).

Bard, Y., *Nonlinear Parameter Estimation*, Academic Press, New York (1974).

Buckley, S. E., and M. C. Leverett, "Mechanisms of Fluid Displacement in Sands," *Trans. AIME*, **146**, 107 (1942).

Chang, Y., K. Mohanty, D. Huang, and M. Honarpour, "The Impact of Wettability and Core-Scale Heterogeneities on Relative Permeability," *J. of Pet. Sci. and Eng.*, **18**, 1 (1997).

Chardaire-Riviere, C., G. Chavent, J. Jaffre, J. Liu, and B. J. Bourbiaux, "Simultaneous Estimation of Relative Permeability and Capillary Pressure," *SPE Form. Eval.*, **7**, 283 (1992).

Chen, S., F. Qin, K.-H. Kim, and A. T. Watson, "NMR Imaging of Flow in Porous Media," *AIChE J.*, **39**, 925 (1993).

Chen, S., F. Qin, and A. T. Watson, "Determination of Fluid Saturations During Multiphase Flow Experiments Using NMR Imaging Techniques," *AIChE J.*, **40**, 1238 (1994).

Constantinides, G., and A. Payatakes, "Network Simulation of Steady-State Two-Phase Flow in Consolidated Porous Media," *AIChE J.*, **42**, 369 (1996).

Cook, R., and C.-L. Tsai, "Residuals in Nonlinear Regression," *Biometrika*, **72**, 23 (1985).

Draper, N. R., and H. Smith, *Applied Regression Analysis*, Wiley, New York (1981).

Dullien, F., *Porous Media Fluid Transport and Pore Structure*, Academic Press, New York (1992).

Fulcher, R., T. Ertekin, and C. Stahl, "Effect of Capillary Number and Its Constituents on Two-Phase Relative Permeability Curves," *J. Pet. Tech.*, **37**, 249 (1985).

Johnson, E. F., D. P. Bossler, and V. O. Naumann, "Calculation of Relative Permeability From Displacement Experiments," *Trans. AIME*, **216** (1959).

Kerig, P. D., and A. T. Watson, "Relative Permeability Estimation From Displacement Experiments: An Error Analysis," *SPE Res. Eng.*, **1**, 175 (1986).

Kerig, P. D., and A. T. Watson, "A New Algorithm for Estimating

Relative Permeability Estimation From Displacement Experiments," *Soc. Pet. Eng. J.*, **2**, 103 (1987).
Kulkarni, R. N., and A. T. Watson, "A Robust Technique for Quantification of NMR Imaging Data," *AIChE J.*, **43**, 2137 (1997).
Larson, R., "Derivation of Generalized Darcy Equations for Creeping Flow in Porous Media," *IECF*, **20**, 132 (1981).
Leverett, M. C., "Flow of Oil-Water Mixtures Through Unconsolidated Sands," *Trans. AIME*, **142** (1940).
Leverett, M. C., "Capillary Behavior in Porous Sands," *Trans. AIME*, 152 (1941).
Mejia, G. M., K. K. Mohanty, and A. T. Watson, "Use of In-Situ Saturation Data in Estimation of Two-Phase Flow Functions in Porous Media," *J. Pet. Sci. Eng.*, **12**, 233 (1995).
Mejia, G. M., A. T. Watson, and J. E. Nordtvedt, "Estimation of Three-Phase Flow Functions in Porous Media," *AIChE J.*, **42**, 233 (1996).
Nordtvedt, J. E., G. Mejia, P. Yang, and A. T. Watson, "Estimation of Capillary Pressure and Relative Permeability Functions Centrifuge Experiments," *SPE Res. Eng.*, **8**, 292 (1993).
Nordtvedt, J., H. Urkedal, A. T. Watson, E. Ebeltoft, K. Koltveit, K. Langaas, and I. Øxnevad, "Estimation of Relative Permeability and Capillary Pressure Functions Using Transient and Equilibrium Data From Steady-State Experiments," *Proc. Int. Symp. of Soc. of Core Analysts*, SCA 9418, Stavanger, Norway (1994).
Nordtvedt, J. E., and K. Kolltveit, "Capillary Pressure Curves From Centrifuge Data by Use of Spline Functions," *SPE Res. Eng.*, **6**, 497 (1991).
Nordtvedt, J. E., K. Langaas, A. Sylte, H. Urkedal, and A. T. Watson, "Estimation of Three-Phase Relative Permeability and Capillary Pressure Functions," *Proc. Eur. Conf. on the Mathematics of Oil Recovery (ECMOR V)*, 113, Leoben, Austria (Sept. 3–6, 1996).
Odeh, A. S., "Effect of Viscosity Ratio on Relative Permeability," *Trans. AIME*, **216**, 346 (1959).
Rapoport, L., and W. Leas, "Properties of Linear Waterfloods," *Trans. AIME*, **198**, 139 (1953).
Richmond, P. C., "Estimating Multiphase Flow Functions From Displacement Experiments," PhD Thesis, Texas A&M Univ., College Station (1988).
Richmond, P. C., and A. T. Watson, "Estimation of Multiphase Flow Functions From Displacement Experiments," *SPE Reservoir Eng.*, **5**, 121 (1990).
Rosenbrock, H. H., and C. Storey, *Computational Techniques for Chemical Engineers*, Pergamon Press, Oxford (1966).
Schumaker, L. L., *Spline Functions: Basic Theory*, Wiley, New York (1981).
Sigmund, P., and F. McCaffery, "An Improved Unsteady-State Procedure for Determining the Relative Permeability Characteristics of Heterogeneous Media," *SPEJ*, **169**, 15 (1979).
Slattery, J., "Single-Phase Flow through Porous Media," *AIChE J.*, **15**, 866 (1969).
Slattery, J., "Two-Phase Flow through Porous Media," *AIChE J.*, **16**, 345 (1970).
Tao, T. M., and A. T. Watson, "Accuracy of JBN Estimates of Relative Permeability: Part 1—Error Analysis," *Soc. Pet. Eng. J.*, **24**, 209 (1984).
Watson, A. T., and C. T. Chang, "Characterizing Porous Media with NMR Methods," *Prog. in Nucl. Magn. Res. Spectr.*, **31**, 343 (1997).
Watson, A. T., P. D. Kerig, and R. W. Otter, "A Test for Detecting Rock Property Nonuniformities in Core Sample," *Soc. of Pet. Eng. J.*, **25**, 909 (1985).
Watson, A. T., H. S. Lane, and J. M. Gatens, III, "History Matching With Cumulative Production Data," *J. Pet. Technol.*, **42**, 96 (1990).
Watson, A. T., P. C. Richmond, P. D. Kerig, and T. M. Tao, "A Regression-Based Method for Estimating Relative Permeabilities from Displacement Experiments," *SPE Res. Eng.*, **3**, 953 (1988).
Wellington, S. L., and H. J. Vinegar, "X-Ray Computerized Tomography," *J. of Pet. Tech.*, **39**, 885 (1987).
Whitaker, S., "Advances in Theory of Fluid Motion in Porous Media," *Ind. Eng. Chem.*, **61**(12), 14–28 (1969).
Whitaker, S., "Flow in Porous Media: A Theoretical Derivation of Darcy's Law," *Transport in Porous Media*, **16**, 3 (1986a).
Whitaker, S., "Flow in Porous Media: II. The Governing Equations for Immiscible, Two-Phase Flow," *Transport in Porous Media*, **16**, 105 (1986b).
Wilkinson, D., "Percolation Model of Immiscible Displacement in the Presence of Buoyancy Forces," *Phys. Rev. A.*, **30**, 520 (1984).
Withjack, E. M., "Computed Tomography for Rock-Property-Determination and Fluid-Flow Visualization," *SPE Form. Eval.*, **3**, 696 (1988).
Withjack, E. M., S. K. Graham, and C.-T. Yang, "Determination of Heterogeneities and Miscible Displacement Characteristics in Corefloods by CT Scanning," *SPE Form. Eval.*, **6**, 447 (1991).

Appendix

Kerig and Watson (1986) developed methodology for determining the accuracy of estimates for properties that are functions of the state (or dependent) quantities. The main features of that method are summarized here.

The method utilizes the well-known linearized covariance analysis (Rosenbrock and Storey, 1966; Bard, 1974) for calculating confidence intervals when a set of unknown parameters, $\vec{\beta}$, is to be estimated by minimization of the objective function given by Eq. 9. If the measurement errors are distributed normally with zero mean and covariance $\boldsymbol{X}$ such that $\boldsymbol{W} = \boldsymbol{X}^{-1}$, errors in parameter estimates are distributed normally with zero mean and covariance $\boldsymbol{P}$ such that

$$\boldsymbol{P} = (\boldsymbol{A}^T \boldsymbol{X}^{-1} \boldsymbol{A})^{-1} \tag{A1}$$

where $\boldsymbol{A}$ is the matrix of sensitivity coefficients, the (i, j)th element of which is

$$\boldsymbol{A}_{ij} = \frac{\partial Y_{si}}{\partial \beta_j}. \tag{A2}$$

Information regarding the accuracy of estimates of the flow *functions* is provided by the covariance matrix of errors in the estimates of the flow functions at any specified value of saturation, which is given by

$$\boldsymbol{V} = \boldsymbol{D}^T \boldsymbol{P} \boldsymbol{D} \tag{A3}$$

where the (i, j)th element of matrix $\boldsymbol{D}$ is the sensitivity of flow function i to parameter β_j at the specified saturation. The pointwise confidence intervals are determined using the matrix $\boldsymbol{V}$ at each saturation point and calculating the confidence interval at the specified saturation by

$$f_{ci} = f_i \pm z_{(1+\alpha)/2} \sqrt{V_{ii}} \tag{A4}$$

where f_{ci} is the value at upper and lower confidence intervals around the ith flow function f_i at the specified saturation, α determines the level of confidence, $z_{(1+\alpha)/2}$ is found from the table of standard normal distribution, and V_{ii} is the ith diagonal element of matrix $\boldsymbol{V}$.

There are some important assumptions. The linearized covariance analysis is based on the assumption that the model can be suitably represented as a linear function in the vicinity of the minimum. Also, it is assumed that the relative permeability and capillary pressure representations are the true functions. To satisfy this, we try to use sufficiently large degrees of freedom so that the splines that represent the properties are able to represent any reasonable flow function. It should also be noted that when computed confidence intervals are large, details associated with the regions may not be very meaningful (Rosenbrock and Storey, 1966).

Manuscript received Dec. 23, 1997, and revision received Aug. 7, 1998.